

# Neurochemical characterization of 5-HT<sub>2A</sub>R partial agonists with simultaneous PET-MRI

Journal of Cerebral Blood Flow & Metabolism  
0(0) 1–12  
© The Author(s) 2024  
Article reuse guidelines:  
sagepub.com/journals-permissions  
DOI: 10.1177/0271678X241302937  
journals.sagepub.com/home/jcbfm



Frederick A Bagdasarian<sup>1,\*</sup>, Kristian Larsen<sup>2,3,\*</sup>,  
Hong Ping Deng<sup>1</sup>, Patrick M Fisher<sup>2,4</sup>, Joseph B Mandeville<sup>1</sup> ,  
Christin Y Sander<sup>1</sup> , Hsiao-Ying Wey<sup>1,5</sup>  and  
Hanne D Hansen<sup>1,2</sup> 

## Abstract

Understanding neuromodulatory effects of serotonin 2A receptor (5-HT<sub>2A</sub>R) agonists with diverse pharmacological profiles is relevant to advancing psychedelic-related drug applications. We performed simultaneous positron emission tomography (PET) and pharmacological magnetic resonance imaging (phMRI) in anesthetized nonhuman primates (NHP; N = 3) to examine partial agonists with varying 5-HT<sub>2A</sub>R affinities and selectivity profiles: psilocybin (30, 60, and 90 µg/kg), lisuride (5 µg/kg), and 25CN-NBOH (15 µg/kg). Receptor occupancy was assessed with [<sup>11</sup>C]MDL-100907 PET, and cerebral blood volume (CBV) changes were measured with phMRI. Mixed partial agonists psilocybin and lisuride evoked biphasic CBV responses, whereas the selective 25CN-NBOH produced monophasic CBV increases. Cortical occupancy for psilocybin plateaued at 60 µg/kg (32%), whereas a lower dose of lisuride (5 µg/kg) resulted in similar occupancy (31%). Administration of 25CN-NBOH resulted in lower occupancy (7%) but larger changes in CBV compared to psilocybin and lisuride. The associations between CBV and 5-HT<sub>2A</sub>R occupancy appear linear for lisuride and 25CN-NBOH, but not for psilocybin. We speculate that the temporal and spatial differences in hemodynamic responses of the three agonists could stem from mixed affinity profiles. This work provides an understanding of pharmacological impacts of mixed serotonergic agonists being pursued as therapeutics for psychiatric conditions, offering valuable insights for future drug applications and development strategies.

## Keywords

5-HT<sub>2A</sub> receptor, non-human primates, PET-MRI, pharmacology, psychedelics

Received 6 May 2024; Revised 31 October 2024; Accepted 2 November 2024

## Introduction

Serotonergic psychedelic substances are gaining considerable interest for the treatment of mental health disorders.<sup>1,2</sup> Although classical psychedelic substances like psilocybin, lysergic acid diethylamide (LSD), and mescaline have considerable pharmacology differences and side effects, there exists a primary commonality:

agonism of the serotonin 2A receptor (5-HT<sub>2A</sub>R), which is strongly suggested to mediate psychedelic experiences.<sup>3</sup> Despite the promise of psychedelics as

<sup>1</sup>Athinoula A. Martinos Center for Biomedical Imaging, Department of Radiology, Massachusetts General Hospital, Harvard Medical School, Charlestown, USA

<sup>2</sup>Neurobiology Research Unit, Copenhagen University Hospital, Rigshospitalet, Copenhagen, Denmark

<sup>3</sup>Department of Medicine, Faculty of Health and Medical Sciences, University of Copenhagen, Denmark

<sup>4</sup>Department of Drug Design and Pharmacology, University of Copenhagen, Denmark

<sup>5</sup>Center for the Neuroscience of Psychedelics, Department of Psychiatry, Massachusetts General Hospital, Harvard Medical School, Charlestown, USA

\*Equal contributing authors.

## Corresponding authors:

Hanne D Hansen, Neurobiology Research Unit, Copenhagen University Hospital, Rigshospitalet, Copenhagen, Denmark.  
Email: hannedhansen@gmail.com

Hsiao-Ying Wey, Athinoula A. Martinos Center for Biomedical Imaging, Department of Radiology, Massachusetts General Hospital, Harvard Medical School, 149 13th Street, Charlestown, MA 02129, USA.  
Email: hsiaoying.vey@mgh.harvard.edu

therapeutics, much remains to be elucidated of their acute pharmacology. Most preclinical assessments of pharmacology are in rodents, which may fail to reliably predict effects within humans. Due to similar physiology and anatomical features to humans, non-human primates (NHPs) are a highly informative model for such evaluations.

Positron Emission Tomography (PET) is a state-of-the-art tool for assessing pharmacological drug action *in vivo* and quantifying drug occupancy at target receptors, a key metric to understand and enable clinical translation of drugs.<sup>4</sup> Pharmacological MRI (phMRI) measures hemodynamic changes induced by drug interventions and downstream neuromodulatory action.<sup>5</sup> The ability to link molecular and neurovascular mechanisms with simultaneous PET-MRI allows for an exciting multi-modal approach to characterize compounds beyond drug-receptor binding. For example, our recent study used PET-phMRI to assess drug action at the serotonin 1B receptor and highlighted downstream signaling pathways in a dose-dependent manner of agonist activity.<sup>6</sup> The application of PET-phMRI to characterize 5-HT<sub>2A</sub>R agonists with diverse pharmacological profiles<sup>3,7,8</sup> can infer relevant drug-specific and occupancy-dependent effects on neural hemodynamics.

This work aims to characterize psilocybin, a serotonergic psychedelic with promising clinical application, by assessing 5-HT<sub>2A</sub>R occupancy and hemodynamic response using PET-phMRI in anesthetized NHPs. We also characterized lisuride to offer complementary insights into the effects of a non-psychedelic, non-selective and partial 5-HT<sub>2A</sub>R agonist. Lastly, we assessed 25CN-NBOH, among the most selective 5-HT<sub>2A</sub>R agonists, to pinpoint effects likely specific to 5-HT<sub>2A</sub>R agonism alone.<sup>9</sup> PET was performed with the 5-HT<sub>2A</sub>R radioligand [<sup>11</sup>C]MDL-100907, and phMRI was used to estimate changes in cerebral blood volume (CBV). Regional brain assessments were focused on two primary networks: Default Mode Network (DMN) and a cortical network comprised of sensory, motor, and occipital cortices. The DMN, subcomponents of which are the Precuneus, Anterior and Posterior Cingulate Cortices (ACC, PCC), is active during internalized cognitive processes and routinely implicated in dissociative effects of psychedelics in functional imaging studies.<sup>10,11</sup> Cortical regions investigated were to probe specific areas more directly associated with symptomatic and behavioral outcomes from psychedelics, i.e. visual with hallucinations, sensory with perception of external stimuli, and motor with movement control. We anticipated that receptor occupancy and hemodynamic profiles would dose-dependently co-vary following drug challenges and that 25CN-NBOH would provide context to direct

contributions of 5-HT<sub>2A</sub>R to observed pharmacological profiles of non-selective agonists.

## Materials and methods

### Animal model and preparation

Three male NHPs (weight: 8.7 ± 1.3 kg, age: 6 ± 1.7 years) were used for imaging experiments. NHPs were deprived of food for 12 h prior to imaging. Intramuscular injections of xylazine (0.5–2.0 mg/kg) and ketamine (10 mg/kg) were used for initial anesthetization. NHPs were intubated and maintained at ~1–1.2% isoflurane in oxygen with a vaporizer and controlled flowmeter. All procedures were reviewed and approved by the Institutional Animal Care and Use Committee (IACUC) of Massachusetts General Hospital in accordance with the ARRIVE guidelines and the Guide for the Care and Use of Laboratory Animals (8th edition), ensuring animal welfare.

### Imaging protocol

Anesthetized NHPs were positioned in a 3 T Siemens TIM-Trio with a BrainPET insert (Siemens, Erlangen, Germany) and a custom PET-compatible 8-channel head coil was used for imaging.<sup>12</sup> A high-resolution T1-weighted MPRAGE (TE1/TE2/TE3/TE4 = 1.64/3.5/5.36/7.22 ms, TR = 2530 ms, TI = 1200 ms, flip angle = 7° with 1 mm isotropic resolution) was acquired. NHPs were injected with Ferumoxytol (monocrystalline iron oxide particles (MION); 10 mg/kg) during an Echo Planar Imaging (EPI) sequences with TE/TR = 22/3000 ms, 1.3 mm isotropic resolution. This EPI scan provided fMRI signals prior to and following MION injections, which can be used to estimate baseline (pre-drug challenge) CBV.<sup>13,14</sup> A repeat EPI fMRI scan was then acquired for the rest of the imaging session to capture the hemodynamic response following drug challenges (see following section).<sup>13</sup> PET imaging was conducted with [<sup>11</sup>C]MDL-100907 (6.30 ± 0.25 mCi across experiments) for 120 min. Baseline PET (no drug injection; N = 4) was acquired first. For drug challenge experiments, NHPs were injected with psilocybin (30 µg/kg, N = 2; 60 µg/kg, N = 3; 90 µg/kg, N = 2; injection volume: 8.02 ± 2.81 mL), lisuride (5 µg/kg, N = 2; injection volume: 10 mL), 25CN-NBOH (30 µg/kg, N = 3; injection volume: 3.96 ± 0.31 mL) ~5–10 minutes into fMRI scanning. A sample diagram of imaging protocols is shown in Figure S1. One of the NHPs with a 60 µg/kg psilocybin dose did not have PET imaging (neither baseline nor occupancy) of [<sup>11</sup>C]MDL-100907, only functional imaging was acquired.

Animal physiology was monitored throughout the scan sessions, including heart rate, blood pressure, SpO<sub>2</sub>, respiration rate, and end-tidal CO<sub>2</sub> to determine they remained within normal ranges, assessed by a qualified veterinarian technician. Resting times for NHPs between scans and drug injections were a minimum of 21 days.

### MRI, phMRI data reconstruction and processing

T1 images were denoised, bias-corrected, non-uniformity corrected, and intensity normalized using FreeSurfer.<sup>15</sup> Brain extraction on T1 and EPI images was performed with a combination of FSL BET<sup>16</sup> and AFNI 3dSkullStrip.<sup>17</sup> Slice-timing correction was used to correct EPI-inherent sampling offsets in interleaved EPI acquisitions. Motion correction was performed with FSL MCFLIRT.<sup>18</sup> The NHP INIA19 brain template and NeuroMaps atlas<sup>19</sup> were used for registrations, performed with Advanced Normalization Tools (ANTs),<sup>20</sup> followed by bias-field correction. Data underwent 4 mm FWHM Gaussian smoothing.

CBV changes following drug administration were estimated with open-source imaging software developed at the Martinos Center for Biomedical Imaging, Massachusetts General Hospital (<https://www.nitrc.org/projects/jip>). Signals were fit with gamma variate functions similar to our previous work:<sup>6</sup>

$$S(t) = \left( \frac{t - t_0}{\tau} \right)^\alpha * e^{\alpha * \left( 1 - \frac{t - t_0}{\tau} \right)}$$

Fits were dependent on drug injection time ( $t_0$ ), times corresponding to fMRI signal peaks ( $\tau$ ), and the shape of the function ( $\alpha$ ) relative to each NHP. To be discussed more in the Results, psilocybin and lisuride phMRI were fit with two (biphasic) gamma functions, while 25CN-NBOH was fit with one (monophasic) gamma function. Notation of  $\gamma_1$  refers to decreased CBV ( $CBV_{\gamma_1}$ ), while  $\gamma_2$  refers to increased CBV ( $CBV_{\gamma_2}$ ) at peak signals following drug injections. CBV was calculated with previously used signal conversion methods,<sup>5,13,21</sup> standardized as the percentage difference from baseline. Representative images were generated with Mango image viewer (Research Imaging Institute, University of Texas Health Science Center; <https://mangoviewer.com/>). Please see Supplementary Information for additional details.

### PET data reconstruction and processing

Dynamic PET data was recorded in list mode and corrected for attenuation, scatter, and decay prior to reconstruction. Images were reconstructed using an in-house PET reconstruction pipeline that employed a

3D-OSEM method, and binning with consecutively longer frames ( $6 \times 10$  s,  $3 \times 20$  s,  $6 \times 30$  s,  $5 \times 1$  min,  $3 \times 2$  min,  $5 \times 5$  min,  $7 \times 10$  min). Generated transformation matrices to the template space were applied to PET data. FWHM Gaussian kernel smoothing (2 mm) was applied. Binding Potential ( $BP_{ND}$ ) was calculated using the Multilinear Reference Tissue Model 2<sup>22</sup> implemented in an open-source imaging software (<https://www.nitrc.org/projects/jip>) using the cerebellum reference region,<sup>23</sup> without the vermis as done in other 5-HT<sub>2A</sub>R PET studies.<sup>24,25</sup> Receptor occupancies (percent) were calculated as:

$$Occupancy = \frac{BP_{ND} \text{ (Baseline)} - BP_{ND} \text{ (Blocking)}}{BP_{ND} \text{ (Baseline)}} * 100$$

We investigated anatomical regions within the DMN, comprised of the ACC, PCC and Precuneus, as it is a key network implicated in psychedelic mechanisms in humans.<sup>10,26</sup> Cortical areas of occipital, sensory, and motor cortices were investigated due to their involvement in the symptomatic effects of psychedelics. These regions also have high 5-HT<sub>2A</sub>R expression, the occupancies of which by psilocybin have been investigated previously to provide molecular context to functional imaging studies on psychedelics involving said regions.<sup>27</sup> Metric summaries for these networks (Table 1) were calculated by the summed average of constitutive ROI mentioned above across NHP for each respective drug and dose, and as such are interpreted in terms of trends.

## Results

### Cerebral 5-HT<sub>2A</sub>R availability in NHPs

Regional baseline  $BP_{ND}$  maps were averaged across four [<sup>11</sup>C]MDL100907 scans (two per NHP), and ROI-averaged group values across the four baseline scans are shown in Figure 1. High  $BP_{ND}$  values (i.e., 1.2–1.5) were observed in the precuneus, ACC and PCC and cortical regions of motor, occipital, and sensory cortices. Moderate  $BP_{ND}$  values (i.e., 0.6–1.0) were observed in sub-cortical regions such as the claustrum and putamen, whereas low binding (i.e., 0.2–0.4) was present in the hippocampus, amygdala, and midbrain. Comparable  $BP_{ND}$  values were observed across all baseline NHP PET scans.

### Receptor occupancies and hemodynamics following 5-HT<sub>2A</sub>R agonism

Occupancies and CBV changes following drug administration are shown in Figure 2 and Table 1.

**Table 1.** Summary of occupancies and maximum CBV changes following serotonergic drug injection.

| Dose                                 | Psilocybin                 |                            |                            | Lisuride                  | 25CN-NBOH                  |
|--------------------------------------|----------------------------|----------------------------|----------------------------|---------------------------|----------------------------|
|                                      | 30 $\mu\text{g}/\text{kg}$ | 60 $\mu\text{g}/\text{kg}$ | 90 $\mu\text{g}/\text{kg}$ | 5 $\mu\text{g}/\text{kg}$ | 30 $\mu\text{g}/\text{kg}$ |
| <b>DMN</b>                           |                            |                            |                            |                           |                            |
| Occupancy                            | 3.86 $\pm$ 4.75            | 19.30 $\pm$ 5.61           | 18.70 $\pm$ 12.31          | 25.77 $\pm$ 6.85          | 4.46 $\pm$ 0.75            |
| CBV <sub><math>\gamma_1</math></sub> | -3.12 $\pm$ 0.89           | -6.00 $\pm$ 2.00           | -1.90 $\pm$ 1.73           | -6.80 $\pm$ 2.25          | N/A                        |
| CBV <sub><math>\gamma_2</math></sub> | +3.65 $\pm$ 1.25           | +5.27 $\pm$ 1.75           | +7.01 $\pm$ 1.38           | +10.73 $\pm$ 6.10         | 12.78 $\pm$ 6.72           |
| <b>Cortices</b>                      |                            |                            |                            |                           |                            |
| Occupancy                            | 11.00 $\pm$ 9.39           | 31.83 $\pm$ 5.68           | 28.88 $\pm$ 12.89          | 31.37 $\pm$ 11.19         | 7.11 $\pm$ 3.50            |
| CBV <sub><math>\gamma_1</math></sub> | -3.36 $\pm$ 0.84           | -5.94 $\pm$ 2.19           | -3.08 $\pm$ 1.62           | -5.56 $\pm$ 2.05          | N/A                        |
| CBV <sub><math>\gamma_2</math></sub> | +3.32 $\pm$ 1.49           | +4.11 $\pm$ 1.94           | +5.09 $\pm$ 2.55           | +10.26 $\pm$ 9.67         | 13.44 $\pm$ 4.00           |

DMN is a summed average of ACC, PCC, and Precuneus. Cortices is a summed average of Motor, Sensory, and Occipital cortices. All data are averages and standard deviations across datapoints for included ROI across NHP used for the defined networks, rounded to the nearest hundredth decimal place, represented as percentages. Occupancies below 0%, if observed, were excluded. After thresholding in the Cortices, total datapoints for Psilocybin 30, 90  $\mu\text{g}/\text{kg}$  and Lisuride are N = 6 for Occupancy and CBV; total datapoints for psilocybin 60  $\mu\text{g}/\text{kg}$  for Occupancy are N = 6, for CBV N = 9; total datapoints for 25CN-NBOH are N = 9 for CBV, N = 6 for Occupancy. After thresholding in the DMN, all total datapoints were the same as Cortices, with the exception of 25CN-NBOH N = 3 for Occupancy. Please refer to the method section for the definition of CBV <sub>$\gamma_1$</sub>  and CBV <sub>$\gamma_2$</sub> .

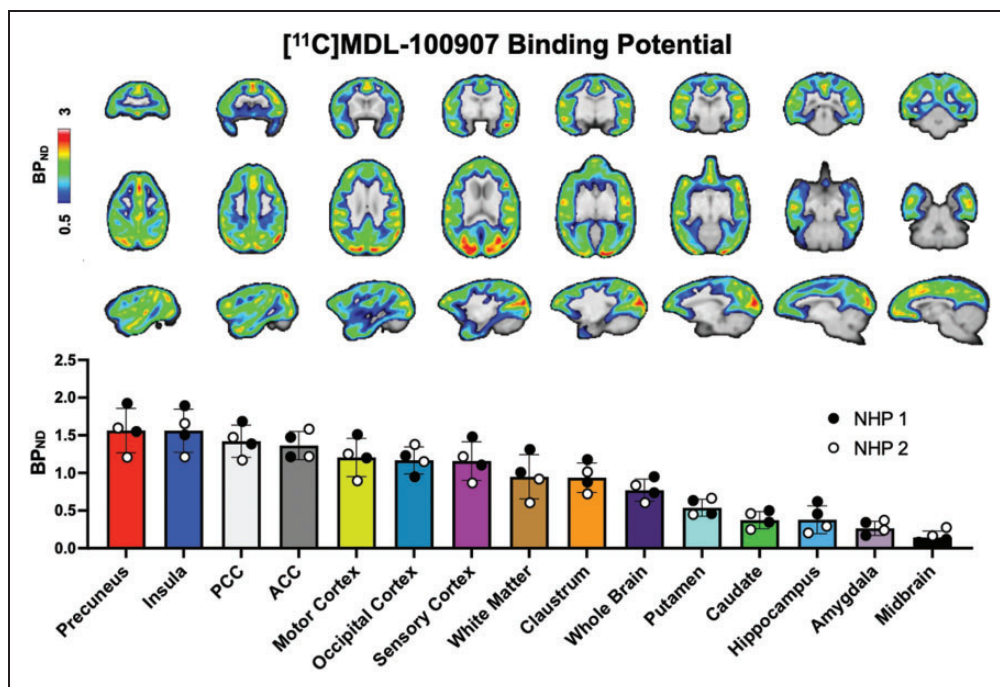


**Figure 1.** Baseline BP<sub>ND</sub> of [<sup>11</sup>C]MDL-100907 in non-human primate (NHP) brains. Representative images are in axial, coronal, and sagittal view. Region-specific BP<sub>ND</sub> are shown from in descending order from highest to lowest observed binding for the ROI sampled. White and black dots represent NHP-specific datapoints.

Psilocybin occupancy was initially observed in occipital regions at 30  $\mu\text{g}/\text{kg}$ , and increased and spread across cortical areas at 60 and 90  $\mu\text{g}/\text{kg}$  doses (Figure 2(a)). Upon visual inspection, hemodynamic responses were observed to be characterized by biphasic (psilocybin, lisuride) or monophasic (25CN-NBOH) gamma profiles (Figure 3) and were modeled as such.

In terms of hemodynamics, psilocybin decreased (Figure 2(b)) and then increased (Figure 2(c)) CBV,

which did not appear fully dependent on BP<sub>ND</sub> distributions. Reductions in CBV were observed in areas with high BP<sub>ND</sub> but also in low-binding sub-cortical areas. The mixed partial agonist lisuride (Figure 2(d) to (f)) also had CBV changes that partially corresponded to BP<sub>ND</sub> and extended to subcortical areas, though cortical distributions of CBV changes from lisuride were more widespread than that of psilocybin. The monophasic hemodynamic profile of the

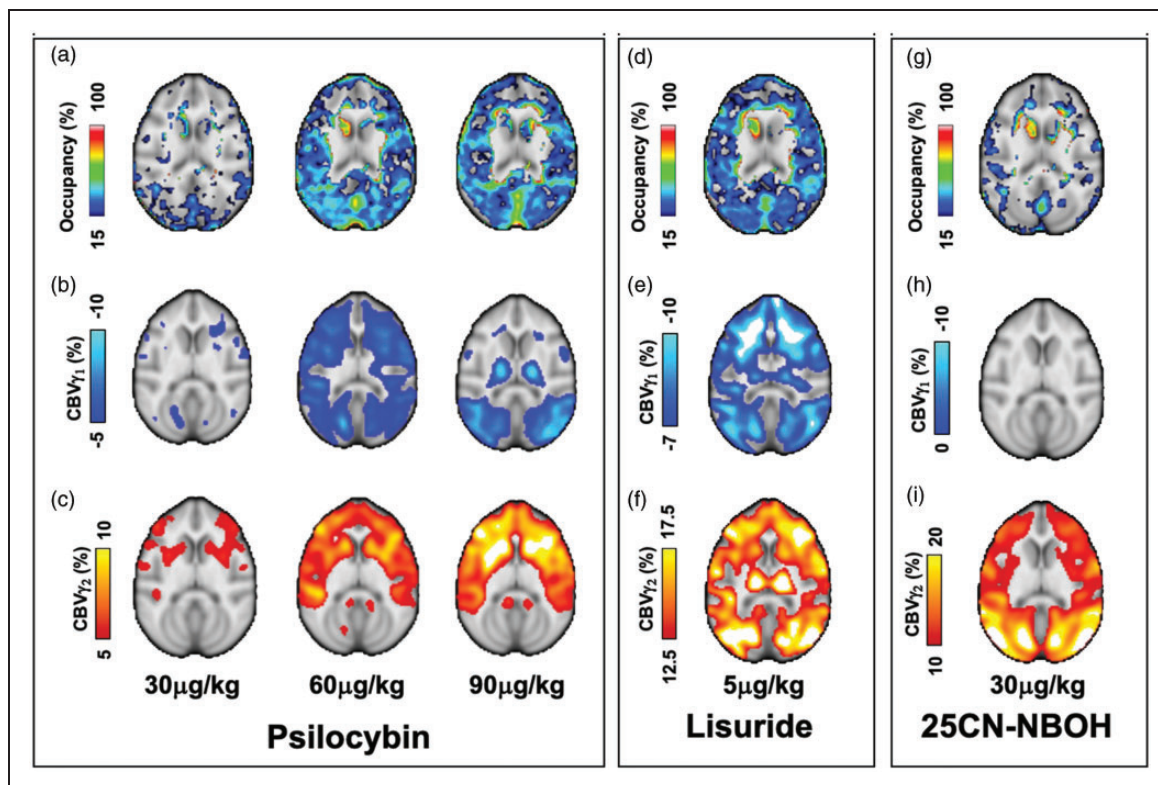


**Figure 2.** Representative axial images of dose-dependent Occupancy (%) and CBV (%) maps from  $\gamma_1$  and  $\gamma_2$  fits for psilocybin (a, b, c), lisuride (d, e, f) and 25CN-NBOH (g, h, i). Only matched pairs of PET-MRI are included, see Supplementary Information for individual NHP maps.

high-affinity agonist 25CN-NBOH indicated only increased CBV (Figure 2(i)) which closely corresponds to baseline  $BP_{ND}$  distributions (Figure 1) but with low occupancy (Figure 2(g)).

Spatial distributions appeared to be dependent on drug and dose. For psilocybin, the spatial distribution of CBV change across dosages of 30, 60, and 90  $\mu\text{g}/\text{kg}$  is similar, with more pronounced effects at higher dosages. Magnitude  $CBV_{\gamma_1}$  was higher in the posterior regions of the brain, whereas  $CBV_{\gamma_2}$  shows more anterior activation. In the case of lisuride, both  $CBV_{\gamma_1}$  and  $CBV_{\gamma_2}$  share similar spatial profiles in cortical and sub-cortical areas. Similarly to psilocybin,  $CBV_{\gamma_1}$  exhibited more posterior decreases. For 25CN-NBOH, there is a wide spatial distribution in  $CBV_{\gamma_2}$  throughout the brain, the larger intensities of which overlap quite well with baseline  $BP_{ND}$  (Figure 1). We also note observable overlap in the  $CBV_{\gamma_2}$  profiles of lisuride and 25CN-NBOH showing slightly more pronounced intensities in the posterior regions of the brain. The notably distinct *and* similar spatial patterns for each drug, particularly in the  $CBV_{\gamma_2}$  profiles, could underscore the pharmacological mechanisms of action among these compounds and will be commented on further in the Discussion.

Representative average bi- or monophasic profiles of cerebral CBV are shown in Figure 3. Dose-dependent profiles are evident for psilocybin. CBV following 30  $\mu\text{g}/\text{kg}$  psilocybin returned to baseline levels approximately 35 minutes post-injection, whereas 60 and 90  $\mu\text{g}/\text{kg}$  doses were nearly, but not yet, at baseline after 70 minutes. For lisuride, whole-brain CBV remained elevated throughout the scan duration. Lisuride scans showed similar peak CBV, however, temporal profiles between the scans were divergent at terminal phases of the scan (Figure S2). The monophasic 25CN-NBOH effect peaked around 10 minutes post-injection and returned to baseline approximately 45 minutes post-injection.

Summaries of average occupancies and maximum CBV changes in 5-HT<sub>2A</sub>R dense networks are shown in Table 1, consisting of summed averages of anatomical regions within the DMN and cortices. Psilocybin increased the average  $CBV_{\gamma_2}$  at each dose but occupancy plateaued at 60  $\mu\text{g}/\text{kg}$ . Lisuride administration resulted in larger occupancy and CBV change compared to psilocybin. 25CN-NBOH had the lowest occupancy but the largest  $CBV_{\gamma_2}$ . Representative graphical illustrations are in Supplementary Information (Figure S3). We also report occupancy and CBV

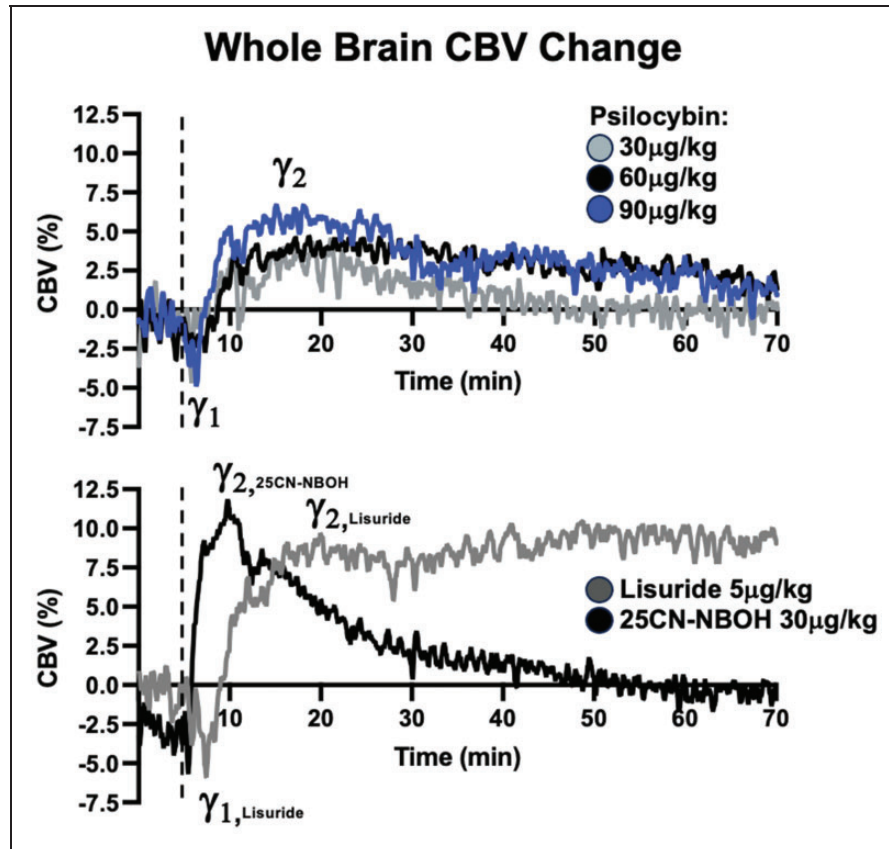


**Figure 3.** Longitudinal cerebral CBV profiles from serotonergic drug challenges, averaged across drug and dose. Dashed lines represent time of drug injection normalized to the 5-minute timepoint.

maps and ROI-extractions for individual NHP in Supplementary Information (Figures S6–S9), which indicate similar drug and dose-dependent trends on a case-by-case basis to those mentioned above for group and dose averages.

#### Assessment of trends between receptor occupancy and hemodynamic changes

We also assessed potential trends or associations between outcome parameters within the networks defined and NHPs (Figure 4, S4) with the hypothesis that more receptor activation, i.e., higher occupancy, would result in stronger hemodynamics. Due to limited animal numbers, this analysis necessitated multiple, non-independent data from the same animals in different ROI which may inflate association strengths ( $R^2$ ) due to within-animal covariance. As such, while we note  $R^2$  in Figures 4, S4, general trends and slopes are more appropriate to discuss in this context to compare drugs as they relate to CBV and occupancy.

Within the cortical network (Figure 4(a)), there was a weak negative trend between  $CBV_{\gamma_1}$  changes and

occupancy (slope =  $-0.04$ ) for psilocybin scans. Lisuride had an interesting and potentially strong trend between occupancy and  $CBV_{\gamma_1}$  (Table 1). At lower receptor occupancy by lisuride (20%) magnitude  $CBV_{\gamma_1}$  was large ( $-9\%$ ), but as occupancy increased (40 to 45%) magnitude  $CBV_{\gamma_1}$  became considerably weaker ( $-3$  to  $-4\%$ ). Regarding occupancy and  $CBV_{\gamma_2}$  (Figure 4(b)), psilocybin had a very weak positive trend (slope =  $0.02$ ), while moderate positive trends were observed for lisuride (slope =  $0.36$ ) and 25CN-NBOH (slope =  $0.72$ ) with increasing occupancy. The DMN ROI had results consistent with cortical findings (Figure S4). Summarily, trends between CBV and occupancy were more easily identifiable for lisuride and 25CN-NBOH, while trends from psilocybin data were more ambiguous.

#### Discussion

This study outlines the use of PET-phMRI in providing molecular information on neurovascular mechanisms relevant to serotonergic and psychedelic substances. We highlight dose-specific occupancies of 5-HT<sub>2A</sub>R

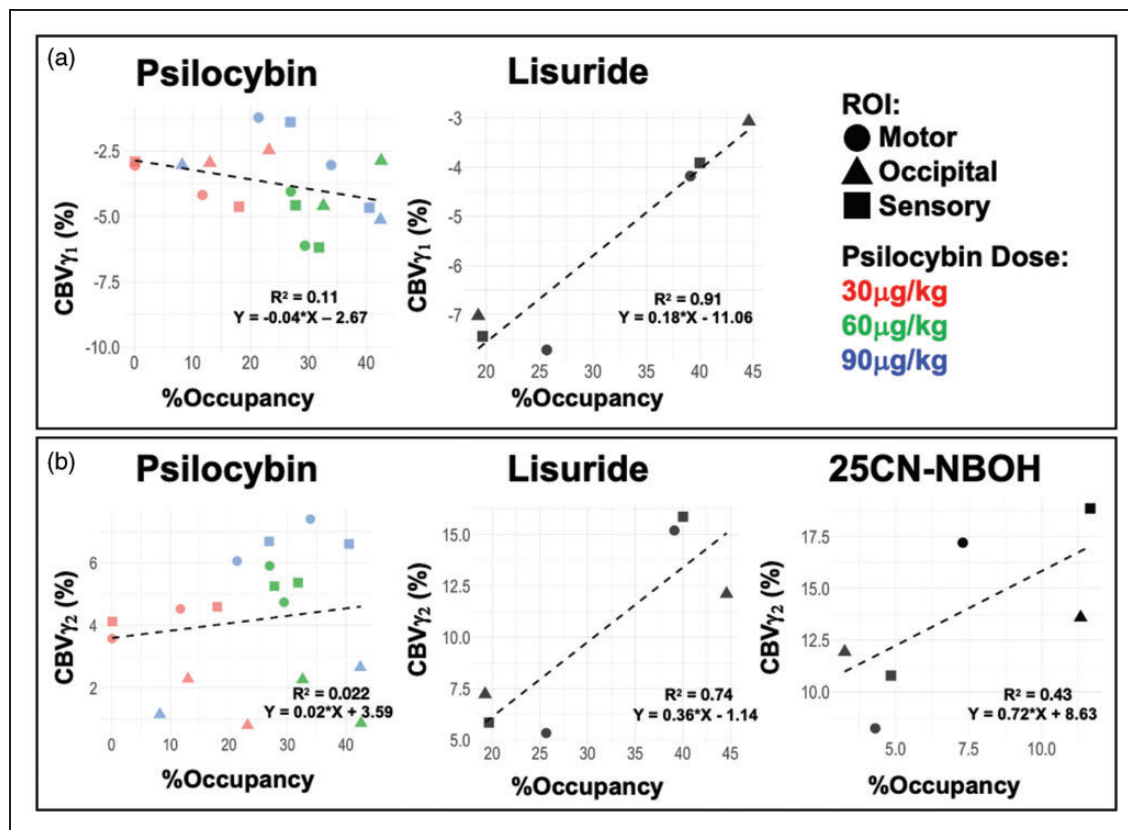


**Figure 4.** Assessment for trends between receptor occupancy (%) and CBV (%) changes for  $\gamma_1$  (a) and  $\gamma_2$  (b) in cortical regions. Datapoints with occupancies below 0%, if observed, were excluded. Total number of datapoints: Psilocybin N = 18; Lisuride N = 6; 25CN-NBOH N = 6.

and influence on CBV by serotonergic agonists of varying affinity and psychedelic potential. Our assessments demonstrate that the mixed agonists psilocybin and lisuride are characterized by biphasic hemodynamic functions, which may be attributable to excitatory-inhibitory processes. Conversely, the non-mixed, highly selective 5-HT<sub>2A</sub>R agonist 25CN-NBOH is characterized by monophasic profiles, which could be purely excitatory. Potential trends between occupancy and hemodynamics were investigated, of which fairly strong linear trends were observed for lisuride and 25CN-NBOH, but not psilocybin.

Prior to drug challenges, we note high baseline binding in DMN regions (ACC, PCC, Precuneus) corresponding to ROIs implicated in the dissociative action of psychedelic substances in human functional imaging studies.<sup>10,11,28</sup> High baseline 5-HT<sub>2A</sub>R expression in cortical areas such as the occipital, sensory, and motor cortices were also observed, each of which are implicated in the symptomatic manifestations of psychedelic drugs, i.e., visual hallucinations and altered perception of external stimuli. These results support our focused assessments on these regions and networks.

#### 5-HT<sub>2A</sub>R occupancy by psilocybin

Our exploration of 5-HT<sub>2A</sub>R occupancy by psilocybin provides important context to its molecular actions *in vivo*. Our data suggests that psilocybin occupancy may plateau at 60  $\mu\text{g}/\text{kg}$  in NHPs (Table 1, Figure S3). This should, however, be viewed with caution due to current animal numbers, the standard deviation of the observed 90  $\mu\text{g}/\text{kg}$  mean, and CBV $\gamma_2$  for psilocybin peaking at 90  $\mu\text{g}/\text{kg}$  (Table 1). Additional studies are planned to confirm these observations.

In any case, average occupancy by psilocybin (Table 1) tends to be higher in the cortices than the DMN. If regionally specific occupancies are occurring, this could indicate that high 5-HT<sub>2A</sub>R density ROI across the DMN and cortex could be delineated to provide a more unique window for examining molecular actions of psychedelics in separate domains *in vivo*, and/or that affinities to, or molecular conformation of, 5-HT<sub>2A</sub>R across the brain may vary. Though regional variability from initial substance uptake could affect measurement uniformity, i.v. administration of psilocybin has been reported to induce peak plasma psilocin concentrations in as fast as 1.9 minutes,<sup>29</sup> and we

anticipate this is not a major contributing factor to ROI heterogeneity. Initial PET uptake (~5 min after drug challenge) may be sensitive to this variability due to non-equilibrium conditions of free tracer levels, but we expect this to be minimal and that the 2-hour dynamic PET data should mitigate transient effects. Measurement variance could likely then be from the current sample size.

A pertinent reference point comes from Donovan et al. (2020), which evaluated a 64  $\mu\text{g}/\text{kg}$  i.v. dose in a pig with [ $^{11}\text{C}$ ]Cimbi-36 PET, reporting whole-brain occupancy of 67%.<sup>30</sup> The relative differences in occupancy between our findings and Donovan et al. may stem from different PET radioligands, i.e., [ $^{11}\text{C}$ ]Cimbi-36 is an agonist ligand<sup>31</sup> theoretically biased toward 5-HT<sub>2A</sub>R receptors in their active state, whereas [ $^{11}\text{C}$ ]MDL-109007, an antagonist PET radioligand<sup>23</sup> which binds to inactive and active 5-HT<sub>2A</sub>R. Furthermore, it's important to acknowledge that Donovan et al.'s utilization of a single pig as the experimental subject makes comparisons across diverse mammalian cohorts difficult. Contextualizing to human pharmacology, we address methodological disparities. While oral administration prevails in human studies, our i.v. administration allows for a meaningful comparison. An oral dose of ~15 mg psilocybin is roughly equivalent to our lowest i.v. dose of 30  $\mu\text{g}/\text{kg}$  when adjusted for body weight and may be considered a "moderate dose."<sup>32</sup> Madsen et al.'s escalating oral dose study (2019) showed a plateau in observed receptor occupancy of 65–70% (model estimated maximum occupancy of 77%) with the use of [ $^{11}\text{C}$ ]Cimbi-36.<sup>33</sup> Drawing on Barrett et al.'s recent work (2022),<sup>27</sup> subjects received an oral dose of 10 mg/70 kg (~140  $\mu\text{g}/\text{kg}$ ) and reported an average occupancy of ~40–45% in motor, sensory, and occipital cortices, much closer to our occupancies at our highest dose. We thus have support for our reported plateaued occupancy profile and corresponding magnitudes relative to PET imaging protocols. Discrepancies between our and previous work could be attributable to inter-species differences and inter-subject variability.

### Contextualizing the biphasic hemodynamic responses of mixed agonists

Observance of biphasic signal profiles lends support to the pHMRI technique for directly quantifying drug challenges *in vivo*, as we can assess the time-varying nature of hemodynamics and what extent those fluctuations may depend on receptor occupancies when combined with PET. Doing so may allow for the identification of physiological biomarkers that could inform the development of neurovascular models (i.e., CBV as a function of occupancy; duration of CBV

peak modulations, etc.).<sup>34</sup> Regarding CBV temporal profiles (Figure 3), we observed evidence for dose-dependent trends toward baseline levels for psilocybin. Average sustained elevation of CBV from lisuride could indicate prolonged molecular and/or vascular action, or nonspecific or metabolite-induced secondary effects. Figure S2 shows between-subject variability in CBV response, however, where one NHP had prolonged elevations and the other showed temporal response more similar to those observed in the psilocybin group. With limited sample size in the lisuride group, mechanistic speculation must be made with caution and will be verified with follow up experiments. Though temporal profiles were distinct, both do exhibit general biphasic profiles as a common observance of these mixed agonists drug injection.

Biphasic signal responses from multi-receptor mechanisms and inhibitory-excitatory action have been reported from electrical stimulation at the cellular level.<sup>35</sup> This is broadly translatable to functional and vascular imaging techniques in preclinical imaging experiments on the interactions of inhibitory and excitatory neurons.<sup>36</sup> Mixed affinities of psilocybin and lisuride are well documented. Reports on psilocybin/psilocin (NIMH Psychoactive Drug Screening Program database: <https://pdsp.unc.edu/databases/pdsp.php>) list affinities at 5-HT<sub>2A</sub>R around  $K_i = 14\text{--}25$  nM, 5-HT<sub>1A</sub>R  $K_i = 49$  nM, and 5-HT<sub>2C</sub>R  $K_i = 10$  nM, and Madsen and colleagues did estimate psilocybin's 5-HT<sub>2A</sub>R affinity to be 10 nM using *in vivo* [ $^{11}\text{C}$ ]Cimbi-36 PET in humans.<sup>33</sup> Lisuride has even higher serotonin receptor affinities: 5-HT<sub>2A</sub>R  $K_i = \sim 3.5$  nM; 5-HT<sub>1A</sub>R  $K_i = 2.7$  nM; 5-HT<sub>2C</sub>R  $K_i = 13.1$  nM, in addition to strong dopamine D<sub>2</sub> receptor (D2R) affinity ( $K_i = \sim 0.8$  nM). These pharmacological profiles point to a more complicated paradigm of agonist-induced deviation from pre-drug physiology that could correspond to mixed excitatory and inhibitory responses. Mechanistically, 5-HT<sub>2A</sub>R activation via agonism induces neuronal excitation through elevated AMPA receptor input (glutamatergic transmission) to cortical pyramidal neurons,<sup>37</sup> and these enhancements may be increasingly "asynchronous" in the context of psychedelic 5-HT<sub>2A</sub>R agonists.<sup>38</sup> Inhibitory effects, on the other hand, upon 5-HT<sub>2A</sub>R activation may be from their presence on GABAergic interneurons in cortical circuits.<sup>39</sup> 25CN-NBOH, however, is among the most selective 5-HT<sub>2A</sub>R agonists<sup>47</sup> and had only monophasic CBV. This could suggest that inhibitory action from 5-HT<sub>2A</sub>R agonism is dominated by its excitatory action on pyramidal neurons and is a main driver of elevated CBV. We hypothesize, then, that biphasic profiles observed here may be a consequence of non-selective action/affinities to receptors besides 5-HT<sub>2A</sub>R that promote substantial



inhibitory action, such as 5-HT<sub>1A</sub>R or 5-HT<sub>2C</sub>R (psilocybin) and D<sub>2</sub>R (lisuride), that correspond to the initial CBV reductions.

Carhart-Harris and Nutt have suggested that serotonergic-mediated behavioral outcomes may be constituted by a “bipartite” system.<sup>40</sup> Previous animal studies have suggested that the head-twitch response (HTR) in rodents induced by psilocybin has a bell-shape with an ascending phase associated with 5-HT<sub>2A</sub>R-mediated excitatory action followed by a descending phase associated with 5-HT<sub>1A</sub>R and 5-HT<sub>2C</sub>R-mediated inhibitory-sedation action,<sup>41,42</sup> though our results present evidence that inhibitory (reduced CBV) followed by excitatory (increased CBV) occurs. Regardless, this purported dynamic relation may be a potential explanation for biphasic hemodynamic responses as inhibitory followed by excitatory action induced by mixed serotonergic agonists like psilocybin. D<sub>2</sub>R agonism, too, is inhibitory and has previously been reported to reduce CBV in similar phMRI experiments for high affinity D<sub>2</sub>R agonists,<sup>34,43</sup> and could account for the reduced CBV observed initially for lisuride. We propose for future studies on 5-HT<sub>2A</sub>R to include blocking experiments using 5-HT<sub>1A</sub>R, 5-HT<sub>2C</sub>R receptor antagonists to investigate their role more directly in biphasic hemodynamics of psilocybin, while for lisuride the inclusion of blocking studies with dopaminergic compounds would also be of relevant interest.

### *The pharmacology of lisuride compared to psilocybin*

Lisuride was studied as a non-psychedelic, the understanding of which may be beneficial for probing serotonergic substances without adverse (i.e., hallucinogenic) effects in clinical populations. Average occupancy, CBV<sub>γ1</sub>, and CBV<sub>γ2</sub> for lisuride (Figure 3, Table 1) were greater than for 60 and 90 μg/kg psilocybin doses, which could be attributable to its higher receptor affinities previously mentioned. We theorize that the combined higher and mixed affinities of lisuride in both the serotonin and dopamine receptor systems may create an additive response that contributes to more intense CBV changes overall when contrasted to psilocybin.

Previous PET/MRI studies have reported that receptor availability and CBV can be modeled depending on the level of neurovascular coupling.<sup>6,43,44</sup> Magnitude CBV<sub>γ1</sub> of lisuride was large at lower occupancy, but as occupancy increases the CBV<sub>γ1</sub> becomes weaker (Figure 4). At the same time, CBV<sub>γ2</sub> increased in magnitude with occupancy. The estimated association suggests a potentially tight linear coupling of these metrics. Although conjectural, perhaps some inhibitory dopaminergic effects induced by lisuride are being

overruled by 5-HT<sub>2A</sub>R driven excitatory effects on CBV<sub>γ1</sub> as higher localized occupancies manifest. High mixed affinities across serotonin and dopamine receptors are also reported for lysergic acid diethylamide (LSD), which is structurally very similar to lisuride. It has been suggested that the high affinity of LSD to dopamine receptors may be a key factor in its distinctively unique symptoms of stimulated behavior.<sup>45,46</sup> A recent study indicated that functional connectivity (regional hemodynamic correlations) in dopamine and serotonin receptor-enriched regions not only correlated to subjective impacts but also differentially modulated inter-network correlations following LSD exposure.<sup>47</sup> Though this cannot be a 1:1 comparison, the effects of multi-receptor domains of mixed-agonists such as LSD and lisuride lend support to our inference of complicated hemodynamic modulations that extend beyond 5-HT<sub>2A</sub>R activity.<sup>32</sup>

In contrast to observed trends between CBV and occupancy for lisuride (Figure 4), 5-HT<sub>2A</sub>R occupancy was surprisingly not predictive of CBV changes from psilocybin. This is visualized by cortical CBV<sub>γ2</sub> trends following psilocybin, which appear very low in the occipital cortex in spite of broad occupancies ranging from 7 to over 40%. We speculate whether the affinity of psilocybin is not high enough to elicit the CBV<sub>γ2</sub> seen with lisuride and 25CN-NBOH, and that the multi-modality of the drug causes less pronounced negative and positive CBV changes. Future studies focusing on such trends or correlations with lisuride and psilocybin at other targets (serotonin, dopamine receptors) with blocking experiments and larger sample sizes could validate our hypotheses on additive/competing neuromodulatory effects therein to provide additional context.

### *Probing direct contributions of 5-HT<sub>2A</sub>R with 25CN-NBOH*

As one of the most selective 5-HT<sub>2A</sub>R agonists,<sup>48</sup> the inclusion of 25CN-NBOH may help to identify pharmacological profiles specific to 5-HT<sub>2A</sub>R agonism. We anticipated a higher occupancy at the same dose of psilocybin due to its higher affinity for 5-HT<sub>2A</sub>R ( $K_i = 2.4$  nM)<sup>48</sup> and low off-target binding. However, at 30 μg/kg we observed comparable occupancy between 25CN-NBOH and psilocybin (Table 1). At the same time, 25CN-NBOH had much larger CBV<sub>γ2</sub> than that of psilocybin despite having similar occupancy to psilocybin at the same dose. It could be that 25CN-NBOH has much higher efficacy at 5-HT<sub>2A</sub>R than psilocybin. We did not, however, account for the efficacies of substances used in this study. Additionally, 25CN-NBOH had comparable CBV<sub>γ2</sub> magnitudes to lisuride, despite substantively higher

occupancies for lisuride (~25–31%) at a much lower dose of 5 µg/kg. And, like lisuride, a positive trend (Figure 4) was observed between occupancy and  $CBV_{\gamma_2}$  for 25CN-NBOH. These results may indicate that 5-HT<sub>2A</sub>R occupancy could model  $CBV_{\gamma_2}$  response for 25CN-NBOH and lisuride, but not psilocybin. In brief, it appears that 25CN-NBOH can elicit strong impacts on hemodynamics at low receptor occupancies, and its monophasic  $CBV_{\gamma_2}$  implies biphasic hemodynamic profiles reported earlier could be due to mixed and/or non-selective affinities of psilocybin and lisuride outside of 5-HT<sub>2A</sub>R and competing inhibitor-excitatory mechanisms.

### Study limitations

Anesthesia was induced via ketamine injections followed by isoflurane, but functional imaging of NHP under anesthesia does not impede fruitful comparisons to human functional imaging.<sup>49</sup> Ketamine may have some affinity for active 5-HT<sub>2A</sub>R sites but does not act as a partial agonist at those sites,<sup>50</sup> though it has been suggested to induce “enhancement” of 5-HT<sub>2A</sub>R signaling as reported in *ex vivo* arterial tissue samples.<sup>51</sup> A report by Matsunaga and colleagues noted that isoflurane only resulted in a ~4% signal inhibition of 5-HT<sub>2A</sub>R.<sup>52</sup> While psilocybin may impact GABA transmission and functional signals, isoflurane’s influence on GABA receptors is not significant.<sup>53</sup> I.v. administration was used, yet these drugs are typically administered peroral. However, previous studies in humans administering psilocybin i.v. support this method as it produces acute psychedelic experiences.<sup>54</sup> Animal models are not perfect 1:1 comparisons to humans, but NHPs are the most translational animal model and allow easier assessments of compounds not currently available for human use, like 25CN-NBOH, in the development of novel 5-HT<sub>2A</sub>R-based therapeutics. [<sup>11</sup>C]MDL-100907 is an antagonist radiotracer, which binds to inactive and inactive 5-HT<sub>2A</sub>R, and may yield different occupancies from agonists radioligand such as [<sup>11</sup>C]Cimbi-36.<sup>33</sup> We were unable to measure radioligand specific molar activity at the time of experimentation. Due to this, the quantity of cold mass (non-radiolabeled) compound that may have been injected with the radioligand, which could influence occupancy measures, is not known. Future experiments using [<sup>11</sup>C]MDL-100907 will include specific molar activity measurements to effectively control for and measure this variable. Though statistical tests could not be performed due to low animal numbers, our results indicate distinct pharmacological trends at the neurovascular level that provide dose-dependent information on vascular changes for each drug, and

potential indicators for receptor-hemodynamic modeling for lisuride and 25CN-NBOH.

### Conclusions

We report distinct neuromodulatory effects of partial agonists with mixed or high affinity to 5-HT<sub>2A</sub>R with simultaneous PET-phMRI. Biphasic hemodynamics appear as a feature of mixed-agonists psilocybin and lisuride, and CBV effects as a function of dose and/or serotonergic agonist choice can provide excellent complimentary physiological markers to occupancy of 5-HT<sub>2A</sub>R. Results from low doses (30 µg/kg psilocybin, 5 µg/kg lisuride) could provide useful information at the early stages of preclinical/clinical studies where low receptor occupancy is preferred or necessary. Our findings enhance the understanding of the *in vivo* pharmacology of serotonergic drugs with and without psychedelic effects, offering valuable insights for future therapeutic applications and drug development strategies. Future studies would benefit from assessing the impacts of selective dopamine and/or 5-HT<sub>2C</sub>R, 5-HT<sub>1A</sub>R antagonists as pretreatment prior to the injections of psilocybin or lisuride. The inclusion of additional non-selective agonists and psychedelic substances (LSD) is also warranted to identify potential imaging signatures of psychedelic-specific mechanisms.

### Funding

The author(s) disclosed receipt of the following financial support for the research, authorship, and/or publication of this article: Pilot Funding from the Athinoula A. Martinos Center for Biomedical Imaging, Department of Radiology, Massachusetts General Hospital. HDH and the psilocybin work was supported by the BBRF Young Investigator grant and Lundbeck Foundation (R293-2018-738). FB is supported by the NIH training grant 5T32AG66592-2. Additional funding was provided by NIH Shared Instrument Grants: S10RR017208, S10RR026666, S10RR022976, S10RR019933, and S10RR023401, S10OD023517.

### Acknowledgements

We thank Helen Deng for all veterinary care and assistance in NHP preparation prior to and physiological monitoring during imaging and drug injections. We thank Shirley Hsu, Oliver Ramsey, and Grae Arabasz for their technical expertise and experimental assistance in setting up PET/MRI experiments.

### Declaration of conflicting interests

The author(s) declared the following potential conflicts of interest with respect to the research, authorship, and/or publication of this article: The authors have no competing interests to declare. At the time of submission HDH is employed by H. Lundbeck A/S.


## Authors' contributions


FB and KL analyzed the neuroimaging data and drafted the manuscript. HDH conceptualized the study and performed the original imaging experiments. JBM developed the analytical process used for NHP data analysis. HYW, CYS, PMF, and HDH provided consultations on methodologies used for data analysis, results interpretations, and discussions. All authors contributed to reviewing and editing the manuscript.

## ORCID iDs

Joseph B Mandeville  <https://orcid.org/0000-0002-4113-5396>

Christin Y Sander  <https://orcid.org/0000-0001-6003-8615>

Hsiao-Ying Wey  <https://orcid.org/0000-0002-1425-8489>

Hanne D Hansen  <https://orcid.org/0000-0001-5564-7627>

## Supplementary material

Supplemental material for this article is available online.

## References

- Krediet E, Bostoen T, Brekxema J, et al. Reviewing the potential of psychedelics for the treatment of PTSD. *Int J Neuropsychopharmacol* 2020; 23: 385–400.
- Reiff CM, Richman EE, Nemeroff CB, et al. Psychedelics and psychedelic-assisted psychotherapy. *Am J Psychiatry* 2020; 177: 391–410.
- López-Giménez JF and González-Maeso J. Hallucinogens and serotonin 5-HT<sub>2A</sub> receptor-mediated signaling pathways. *Curr Top Behav Neurosci* 2018; 36: 45–73.
- Matthews PM, Rabiner EA, Passchier J, et al. Positron emission tomography molecular imaging for drug development. *Br J Clin Pharmacol* 2012; 73: 175–186.
- Jenkins BG. Pharmacologic magnetic resonance imaging (phMRI): imaging drug action in the brain. *Neuroimage* 2012; 62: 1072–1085.
- Hansen HD, Mandeville JB, Sander CY, et al. Functional characterization of 5-HT<sub>1B</sub> receptor drugs in non-human primates using simultaneous PET-MR. *J Neurosci* 2017; 37: 10671–10678.
- Darmon M, Al Awabdh S, Emerit MB, et al. Insights into serotonin receptor trafficking: cell membrane targeting and internalization. *Prog Mol Biol Transl Sci* 2015; 132: 97–126.
- Roth BL and Gray JA. Paradoxical trafficking and regulation of 5-HT<sub>2A</sub> receptors by agonists and antagonists. *Brain Res Bull* 2001; 56: 441–451.
- Jensen AA, McCorvy JD, Leth-Petersen S, et al. Detailed characterization of the In vitro pharmacological and pharmacokinetic properties of N-(2-Hydroxybenzyl)-2, 5-Dimethoxy-4-Cyanophenylethylamine (25CN-NBOH), a highly selective and brain-penetrant 5-HT<sub>2A</sub> receptor agonist. *J Pharmacol Exp Ther* 2017; 361: 441–453.
- Carhart-Harris RL, Leech R, Erritzoe D, et al. Functional connectivity measures after psilocybin inform a novel hypothesis of early psychosis. *Schizophr Bull* 2013; 39: 1343–1351.
- Carhart-Harris RL, Muthukumaraswamy S, Roseman L, et al. Neural correlates of the LSD experience revealed by multimodal neuroimaging. *Proc Natl Acad Sci U S A* 2016; 113: 4853–4858.
- Sander CY, Keil B, Chonde DB, et al. A 31-Channel MR brain array coil compatible with positron emission tomography. *Magn Reson Med* 2015; 73: 2363–2375.
- Lu H, Patel S, Luo F, et al. Spatial correlations of laminar BOLD and CBV responses to rat whisker stimulation with neuronal activity localized by fos expression. *Magn Reson Med* 2004; 52: 1060–1068.
- Mandeville JB, Marota JJ, Kosofsky BE, et al. Dynamic functional imaging of relative cerebral blood volume during rat forepaw stimulation. *Magn Reson Med* 1998; 39: 615–624.
- Sled JG, Zijdenbos AP and Evans AC. A nonparametric method for automatic correction of intensity nonuniformity in MRI data. *IEEE Trans Med Imaging* 1998; 17: 87–97.
- Smith SM. Fast robust automated brain extraction. *Hum Brain Mapp* 2002; 17: 143–155.
- Cox RW. AFNI: software for analysis and visualization of functional magnetic resonance neuroimages. *Comput Biomed Res* 1996; 29: 162–173.
- Jenkinson M, Bannister P, Brady M, et al. Improved optimization for the robust and accurate linear registration and motion correction of brain images. *Neuroimage* 2002; 17: 825–841.
- Rohlfing T, Kroenke CD, Sullivan EV, et al. The INIA19 template and NeuroMaps atlas for primate brain image parcellation and spatial normalization. *Front Neuroinform* 2012; 6: 27.
- Avants BB, Tustison N and Johnson H. *Advanced Normalization Tools (ANTs) Release 2.x*. <https://briannaavants.wordpress.com/2012/04/13/updated-ants-compile-instructions-april-12-2012/>. 2014.
- Mandeville JB. IRON fMRI measurements of CBV and implications for BOLD signal. *Neuroimage* 2012; 62: 1000–1008.
- Ichise M, Liow J-S, Lu J-Q, et al. Linearized reference tissue parametric imaging methods: application to [<sup>11</sup>C]DASB positron emission tomography studies of the serotonin transporter in human brain. *J Cereb Blood Flow Metab* 2003; 23: 1096–1112.
- Talbot PS, Slifstein M, Hwang D-R, et al. Extended characterisation of the serotonin 2A (5-HT<sub>2A</sub>) receptor-selective PET radiotracer <sup>11</sup>C-MDL100907 in humans: quantitative analysis, test-retest reproducibility, and vulnerability to endogenous 5-HT tone. *Neuroimage* 2012; 59: 271–285.
- Fischman AJ, et al. Positron emission tomographic analysis of central 5-hydroxytryptamine<sub>2</sub> receptor occupancy in healthy volunteers treated with the novel antipsychotic agent, ziprasidone. *Journal of Pharmacology and Experimental Therapeutics* 1996; 279: 939–947.
- Chow TW, Mamo DC, Uchida H, et al. Test-retest variability of high resolution positron emission tomography (PET) imaging of cortical serotonin (5HT<sub>2A</sub>) receptors in older, healthy adults. *BMC Med Imaging* 2009; 9: 12.
- Madsen MK, Stenbæk DS, Arvidsson A, et al. Psilocybin-induced changes in brain network integrity and segregation correlate with plasma psilocin level and

- psychedelic experience. *Eur Neuropsychopharmacol* 2021; 50: 121–132.
27. Barrett FS, Zhou Y, Carbonaro TM, et al. Human cortical serotonin 2A receptor occupancy by psilocybin measured using [<sup>11</sup>C]MDL 100,907 dynamic PET and a resting-state fMRI-based brain parcellation. *Front Neuroergon* 2021; 2: 784576.
  28. Palhano-Fontes F, Andrade KC, Tofoli LF, et al. The psychedelic state induced by ayahuasca modulates the activity and connectivity of the default mode network. *PLoS One* 2015; 10: e0118143.
  29. Hasler F, Bourquin D, Brenneisen R, et al. Determination of psilocin and 4-hydroxyindole-3-acetic acid in plasma by HPLC-ECD and pharmacokinetic profiles of oral and intravenous psilocybin in man. *Pharm Acta Helv* 1997; 72: 175–184.
  30. Donovan LL, Johansen JV, Ros NF, et al. Effects of a single dose of psilocybin on behaviour, brain 5-HT<sub>2A</sub> receptor occupancy and gene expression in the pig. *Eur Neuropsychopharmacol* 2021; 42: 1–11.
  31. Finnema SJ, Stepanov V, Ettrup A, et al. Characterization of [(11)C]cimbi-36 as an agonist PET radioligand for the 5-HT(2A) and 5-HT(2C) receptors in the nonhuman primate brain. *Neuroimage* 2014; 84: 342–353.
  32. Turton S, Nutt DJ and Carhart-Harris RL. A qualitative report on the subjective experience of intravenous psilocybin administered in an fMRI environment. *Curr Drug Abuse Rev* 2014; 7
  33. Madsen MK, Fisher PM, Burmester D, et al. Psychedelic effects of psilocybin correlate with serotonin 2A receptor occupancy and plasma psilocin levels. *Neuropsychopharmacology* 2019; 44: 1328–1334.
  34. Mandeville JB, Sander CYM, Jenkins BG, et al. A receptor-based model for dopamine-induced fMRI signal. *Neuroimage* 2013; 75: 46–57.
  35. Puig MV, Artigas F and Celada P. Modulation of the activity of pyramidal neurons in rat prefrontal cortex by raphe stimulation in vivo: involvement of serotonin and GABA. *Cereb Cortex* 2005; 15: 1–14.
  36. Moon HS, Jiang H, Vo TT, et al. Contribution of excitatory and inhibitory neuronal activity to BOLD fMRI. *Cereb Cortex* 2021; 31: 4053–4067.
  37. Aghajanian GK and Marek GJ. Serotonin induces excitatory postsynaptic potentials in apical dendrites of neocortical pyramidal cells. *Neuropharmacology* 1997; 36: 589–599.
  38. Aghajanian GK and Marek GJ. Serotonin, via 5-HT(2A) receptors, increases EPSCs in layer V pyramidal cells of prefrontal cortex by an asynchronous mode of glutamate release. *Brain Res* 1999; 825
  39. Jakab RL and Goldman-Rakic PS. Segregation of serotonin 5-HT<sub>2A</sub> and 5-HT<sub>3</sub> receptors in inhibitory circuits of the primate cerebral cortex. *Journal of Comparative Neurology* 2000; 417
  40. Carhart-Harris RL and Nutt DJ. Serotonin and brain function: a tale of two receptors. *J Psychopharmacol* 2017; 31: 1091–1120. Preprint at <https://doi.org/10.1177/0269881117725915>
  41. Liu J, Wang Y, Xia K, et al. Acute psilocybin increased cortical activities in rats. *Front Neurosci* 2023; 17: 1168911.
  42. Shahar O, Botvinnik A, Esh-Zuntz N, et al. Role of 5-HT<sub>2A</sub>, 5-HT<sub>2C</sub>, 5-HT<sub>1A</sub> and TAAR1 receptors in the head twitch response induced by 5-hydroxytryptophan and psilocybin: translational implications. *Int J Mol Sci* 2022; 23
  43. Sander CY, Hooker JM, Catana C, et al. Imaging agonist-induced D<sub>2</sub>/D<sub>3</sub> receptor desensitization and internalization in vivo with PET/fMRI. *Neuropsychopharmacology* 2016; 41: 1427–1436.
  44. Sander CY, Hooker JM, Catana C, et al. Neurovascular coupling to D<sub>2</sub>/D<sub>3</sub> dopamine receptor occupancy using simultaneous PET/functional MRI. *Proc Natl Acad Sci U S A* 2013; 110: 11169–11174.
  45. Marona-Lewicka D, Thisted RA and Nichols DE. Distinct temporal phases in the behavioral pharmacology of LSD: dopamine D<sub>2</sub> receptor-mediated effects in the rat and implications for psychosis. *Psychopharmacology (Berl)* 2005; 180: 427–435.
  46. Borroto-Escuela DO, Romero-Fernandez W, Narvaez M, et al. Hallucinogenic 5-HT<sub>2A</sub> agonists LSD and DOI enhance dopamine D<sub>2R</sub> protomer recognition and signaling of D<sub>2</sub>-5-HT<sub>2A</sub> heteroreceptor complexes. *Biochem Biophys Res Commun* 2014; 443: 278–284.
  47. Lawn T, Dipasquale O, Vamvakas A, et al. Differential contributions of serotonergic and dopaminergic functional connectivity to the phenomenology of LSD. *Psychopharmacology (Berl)* 2022; 239: 1797–1808.
  48. Jensen AA, Halberstadt AL, Märcher-Rørsted E, et al. The selective 5-HT<sub>2A</sub> receptor agonist 25CN-NBOH: structure-activity relationship, in vivo pharmacology, and in vitro and ex vivo binding characteristics of [3H]25CN-NBOH. *Biochem Pharmacol* 2020; 177: 113979.
  49. Wey H-Y, Phillips KA, McKay DR, et al. Multi-region hemispheric specialization differentiates human from nonhuman primate brain function. *Brain Struct Funct* 2014; 219: 2187–2194.
  50. Kapur S and Seeman P. NMDA receptor antagonists ketamine and PCP have direct effects on the dopamine D<sub>2</sub> and serotonin 5-HT<sub>2</sub> receptors – implications for models of schizophrenia. *Mol Psychiatry* 2002; 7: 837–844.
  51. Lin H, Kim JG, Park SW, et al. Enhancement of 5-HT<sub>2A</sub> receptor function and blockade of Kv1.5 by MK801 and ketamine: implications for PCP derivative-induced disease models. *Exp Mol Med* 2018; 50: 1–8.
  52. Matsunaga F, Gao L, Huang X-P, et al. Molecular interactions between general anesthetics and the 5HT<sub>2B</sub> receptor. *J Biomol Struct Dyn* 2015; 33: 211–218.
  53. Sandiego CM, Jin X, Mulnix T, et al. Awake nonhuman primate brain PET imaging with minimal head restraint: evaluation of GABAA-benzodiazepine binding with [<sup>11</sup>C]-Flumazenil in awake and anesthetized animals. *J Nucl Med* 2013; 54: 1962–1968.
  54. Carhart-Harris RL, Erritzoe D, Williams T, et al. Neural correlates of the psychedelic state as determined by fMRI studies with psilocybin. *Proc Natl Acad Sci U S A* 2012; 109: 2138–2143.